Conditions for tighter focusing and higher focal depth of radially polarized vector beam

Xiumin Gao[1*], Qi Wang[2], Maojin Yun[3], Jiancheng Yu[1], Hanming Guo[2], Songlin Zhuang[2]

[1]Electronics and Information College, Hangzhou Dianzi University, Hangzhou 310018, China

[2]University of shanghai for Science and Technology, Shanghai 200093, China

[3]College of Physics Science, Qingdao University, Qingdao 266071, China

[*]Corresponding author: xiumin_gao@yahoo.com.cn

The radially polarized vector beam has attracted much attention recently and was also used to obtain a smaller focal spot. In this paper, highly focusing properties of radially polarized vector beam are investigated by comparing them with those of linearly polarized beam. A condition was found for tighter focusing of radially polarized vector beam. The focal spot of radially polarized vector beam is not always smaller than that of linearly polarized beam. Even if only a longitudinal field component is considered, in fact, the condition for tighter focusing of radially polarized vector beam is very complicated. Therefore, more attention should be paid to the smaller focal spot generation by means of radially polarized vector beam in practical use. In addition, the focal depth of radially polarized beam decreases on increasing numerical aperture under condition of small radius ratio, and increases on increasing radius ratio. The focal depth difference between these two kinds of beams shrinks upon increasing radius ratio and numerical aperture.

Keywords: radially polarized vector beam, focusing properties, vector diffraction theory.

1. Introduction

As a kind of the cylindrical vector beam, radially polarized beam (RPB) has recently gained much interest and attention due to its novel properties and wide applications, such as particle-trapping, optical data storage, laser machining and lithography [1–7]. Especially, the focusing properties of RPB are investigated inventively [8–12]. Kozawa and Sato investigated the strong focusing of higher transverse modes of radially polarized beams [13], which illustrates that the strong longitudinal component forms a sharper spot at the focal point under a high-NA focusing condition. In addition, focusing properties of higher radial modes were also studied systemically by Rashid *et al*. [14]. It was demonstrated both theoretically and experimentally that the introduction of RPB illumination combined with an annular beam illumination exhibits advantages in two aspects [9]. Firstly, it corrects the focus elongation and

splitting in a focused evanescent field associated with a linearly polarized beam, and secondly, it also improves significantly the lateral localization to approximately a quarter of the illumination wavelength, which is less than half of the size that is achievable under linearly polarized beam (LPB) illumination. The effect of apodization on spot size under tight focusing conditions was also studied [15].

   In this paper, highly focusing properties of RPB and LPB are studied to investigate the smaller focal spot generation effect of the RPB beam in detail. It has been found that the condition for tighter focusing of RPB is complicated in fact. On the other hand, focal depth is also a very important parameter in many optical systems and can be used to enhance the performance [16–20]. For example, in high-density optical data storage system, large focal depth makes it easy for the servo system to track. It was found in our investigation that the focal spot of RPB is not always smaller than that of LPB, and the focal depth difference between these two kinds of beams shrinks on increasing numerical aperture. Focusing principle is given in Section 2. Section 3 shows the simulation results and discussion. In addition, comparisons under high-order radial modes are given. The conclusions are summarized in Section 4.

2. Focusing principle of RPB and LPB

In the focusing system, we investigated the incident beam convergence through an objective lens. The focusing principle of RPB has been analyzed recently, and the electric field in the focal region in cylindrical coordinates can be written in the form [12, 21],

$$\mathbf{E_C}(r, \varphi, z) \; = \; E_{CR}\,\mathbf{e_r} + E_{CZ}\,\mathbf{e_z} \tag{1}$$

where $\mathbf{e_r}$ and $\mathbf{e_z}$ are the unit vectors in the radial and propagating directions, respectively. E_{CR} and E_{CZ} are amplitudes of the two orthogonal components, which can be expressed as

$$E_{CR}(r, z) \; = \; A\int_{\theta_1}^{\theta_2} P(\theta)\sqrt{\cos(\theta)}\,\sin(2\theta)\,J_1\!\big(kr\sin(\theta)\big)\exp\!\big(ikz\cos(\theta)\big)\mathrm{d}\theta \tag{2}$$

$$E_{CZ}(r, z) \; = \; 2iA\int_{\theta_1}^{\theta_2} P(\theta)\sqrt{\cos(\theta)}\,\sin^2(\theta)\,J_0\!\big(kr\sin(\theta)\big)\exp\!\big(ikz\cos(\theta)\big)\mathrm{d}\theta \tag{3}$$

where r and z are the radial and longitudinal coordinates of observation point in focal region, respectively. Parameter A is a constant, and k is the wave number. Parameter θ_j ($j = 1, 2$) represents the polar angle corresponding to the optical aperture, namely, $\theta_2 = a\sin(\mathrm{NA})$, and $\theta_1 = a\tan[R\tan(\theta_2)]$, R is the normalized inner radius of the optical aperture by outer radius of the optical aperture, and if $R = 0$ the optical aperture is a circle aperture, else it is an annular aperture. $P(\theta)$ is the pupil function that describes the amplitude of the field in the pupil of the lens which is assumed to be a function

of θ only [12, 14]. The optical intensity of RPB in focal region can be obtained by calculating the square modulus of Eq. (1). It can be seen that the focal pattern of RPB is cylindrical symmetric.

The electric field in the focal region of LPB is expressed in Cartesian coordinates, and if the incident polarization is in x direction, the electric field is in the form [22, 23],

$$\mathbf{E_L}(r, \phi, z) = E_{LX}\mathbf{x} + E_{LY}\mathbf{y} + E_{LZ}\mathbf{z} =$$

$$= \frac{\pi E_0 i}{\lambda}\left\{\left[I_0 + \cos(2\phi)I_2\right]\mathbf{x} + \sin(2\phi)I_2\,\mathbf{y} + 2i\cos(\phi)I_1\mathbf{z}\right\} \tag{4}$$

where $\mathbf{x}$, $\mathbf{y}$, and $\mathbf{z}$ are the unit vectors in the x, y, and z directions, respectively. E_0 is a constant. It is clear that the incident Gaussian beam is depolarized and has three components (E_{LX}, E_{LY} and E_{LZ}). Variables r, ϕ, and z are the cylindrical coordinates of an observation point in focal region. Variables I_0, I_1, and I_2 are [22, 23],

$$I_0 = \int_{\theta_1}^{\theta_2} P(\theta)\sqrt{\cos(\theta)}\,\sin(\theta)\Big(1 + \cos(\theta)\Big)J_0\Big(kr\sin(\theta)\Big)\exp\Big(-ikz\cos(\theta)\Big)d\theta \tag{5}$$

$$I_1 = \int_{\theta_1}^{\theta_2} P(\theta)\sqrt{\cos(\theta)}\,\sin^2(\theta)J_1\Big(kr\sin(\theta)\Big)\exp\Big(-ikz\cos(\theta)\Big)d\theta \tag{6}$$

$$I_2 = \int_{\theta_1}^{\theta_2} P(\theta)\sqrt{\cos(\theta)}\,\sin(\theta)\Big(1 - \cos(\theta)\Big)J_2\Big(kr\sin(\theta)\Big)\exp\Big(-ikz\cos(\theta)\Big)d\theta \tag{7}$$

where k is also the wave number. $J_0(x)$, $J_1(x)$, $J_2(x)$ and are the zero-order, the first--order, and the second-order Bessel functions of the first kind, respectively. In order to make a comparison simple, parameter θ_j ($j = 1, 2$) represents the same polar angle corresponding to the optical aperture, $\theta_2 = a\sin(\text{NA})$ and $\theta_1 = a\tan[R\tan(\theta_2)]$. $P(\theta)$ in Eqs. (5)–(7) has the same meaning as that in Eqs. (2) and (3). Focusing properties of RPB and LPB can be obtained numerically by calculating Eqs. (1) and (4), respectively.

3. Numerical results and discussion

3.1. Transverse focal size comparison between RPB and LPB

Here, the focusing property comparison between RPB and LPB is discussed. Without loss of validity and generality, the pupil function is taken as $P(\theta) = 1$. It should be noted that the size of focal spot is shown as the full width at half maximum (FWHM) in the focal plane, and its unit is k^{-1}, k is the wave number and equals $2\pi/\lambda$, where λ is the wavelength of incident beam. And all the distance units in the tables and figures of this article are also k^{-1}. Table 1 shows the transverse FWHM of focal spot

of focusing LPB and RPB. E_{LY} and E_{LX} indicate the transverse FWHM in x and y coordinate directions in focal region of LPB, respectively. E_C and E_{CZ} give the FWHM of the total field and longitudinal field in focal region of RPB, respectively. It can be seen that the focal spot symmetry of LPB is considerably better determined under condition of higher numerical aperture and larger R. For instance, the FWHM ratio of E_{LX} to E_{LY} is about 2.6 (= 5.30/2.02) for the case of NA = 0.99 and $R = 0.4$. The width of the focal spot is smaller in the direction perpendicular to the initial direction of

T a b l e 1. Transverse FWHM of focal spot of focusing LPB and RPB.

	NA	0.75	0.80	0.85	0.90	0.93	0.96	0.99
$R = 0$	E_{LY}	4.16	3.88	3.62	3.38	3.24	3.10	2.96
	E_{LX}	4.96	4.78	4.66	4.60	4.58	4.60	4.68
	E_C	9.12	7.60	6.04	4.80	4.26	3.80	3.42
	E_{CZ}	3.86	3.60	3.38	3.18	3.06	2.96	2.84
$R = 0.1$	E_{LY}	4.12	3.82	3.56	3.30	3.14	2.94	2.54
	E_{LX}	4.92	4.74	4.62	4.54	4.54	4.56	4.84
	E_C	9.10	7.54	5.98	4.74	4.16	3.68	3.00
	E_{CZ}	3.84	3.60	3.38	3.16	3.04	2.90	2.66
$R = 0.2$	E_{LY}	3.98	3.68	3.38	3.10	2.90	2.66	2.22
	E_{LX}	4.82	4.64	4.52	4.48	4.50	4.66	5.24
	E_C	8.78	7.16	5.58	4.36	3.80	3.26	2.60
	E_{CZ}	3.82	3.56	3.32	3.08	2.94	2.76	2.46
$R = 0.3$	E_{LY}	3.80	3.48	3.20	2.88	2.68	2.44	2.10
	E_{LX}	4.68	4.52	4.44	4.46	4.60	4.90	5.30
	E_C	8.16	6.44	4.96	3.90	3.40	2.92	2.44
	E_{CZ}	3.74	3.46	3.22	2.96	2.80	2.62	2.38
$R = 0.4$	E_{LY}	3.62	3.30	3.02	2.72	2.52	2.32	2.02
	E_{LX}	4.56	4.44	4.40	4.54	4.76	5.10	5.30
	E_C	7.32	5.66	4.38	3.52	3.10	2.74	2.38
	E_{CZ}	3.62	3.36	3.10	2.84	2.70	2.52	2.34
$R = 0.5$	E_{LY}	3.44	3.14	2.86	2.58	2.42	2.22	2.00
	E_{LX}	4.46	4.38	4.44	4.68	4.92	5.22	5.30
	E_C	6.46	4.98	3.98	3.24	2.90	2.62	2.34
	E_{CZ}	3.50	3.24	2.98	2.74	2.60	2.46	2.32
$R = 0.6$	E_{LY}	3.28	3.00	2.74	2.48	2.34	2.16	1.96
	E_{LX}	4.40	4.38	4.50	4.80	5.06	5.26	5.30
	E_C	5.70	4.46	3.64	3.06	2.78	2.54	2.32
	E_{CZ}	3.38	3.12	2.88	2.68	2.54	2.42	2.30
$R = 0.7$	E_{LY}	3.14	2.88	2.64	2.42	2.28	2.14	1.96
	E_{LX}	4.36	4.40	4.58	4.92	5.14	5.28	5.30
	E_C	5.10	4.08	3.40	2.92	2.70	2.50	2.32
	E_{CZ}	3.26	3.02	2.80	2.60	2.50	2.40	2.30

polarization than that in x direction. And the transverse FWHM in y direction decreases more sharply on increasing NA. The FWHM in x direction decreases more slowly, and then increases back on increasing NA under condition of smaller R. However, for larger R, the FWHM in x direction increases continually on increasing NA. The focal spot of RPB has cylindrical symmetry. And under condition of small R, the dependence of FWHM difference between E_C and E_{CZ} on R is not linear, in addition, the dependence of this FWHM difference on NA is also not linea. This article pays more attention to tighter focal spot generation of RPB by comparison with LPB. From Table 1, we can see that the focal spot of RPB is not always smaller than that of LPB, even if only a longitudinal field component E_{CZ} is considered. And for certain case, the FWHM of LPB in y direction may be smaller than that of E_{CZ} even for higher numerical aperture.

For the purpose of presenting the information in a more friendly manner, some important parts of this data table are given graphically. Figure 1**a** illustrates the transverse FWHMs of fields E_{LY}, E_{LX}, E_C, and E_{CZ} for NA = 0.75. It can be seen that the FWHMs of fields E_{LX} and E_C are relatively big, and are smaller for fields E_{LY} and E_{CZ}. When considering the total optical focal spot, in fact, the focusing of RPB does not give a smaller focal spot than LPB, namely, tighter focusing does not appear as usual. Even if only the FWHM of E_{LY} and E_{CZ} is considered, sharper focusing for RPB does not always occur. For small R, FWHM of E_{CZ} is smaller than that of E_{LY}. When R approaches a big value, the FWHM of E_{CZ} is bigger than that of E_{LY}. The FWHMs of fields E_{LY}, E_{LX}, E_C, and E_{CZ} for NA = 0.80 are also given according to Tab. 1. We can see that the condition for sharper focusing of RPB is very complicated even if only E_{LY} and E_{CZ} are considered, because the FWHM ratio of E_{LY} to E_{CZ} fluctuates near 1 on increasing R, and there are three cross points for E_{LY} to E_{CZ} FWHM curves. The FWHM curve of E_C also crosses with that of E_{LY}.

The FWHMs of fields E_{LY}, E_{LX}, E_C, and E_{CZ} under condition of NA = 0.90 are also illustrated in Fig. 2**a**. From this figure, we can see that the FWHM curve cross point
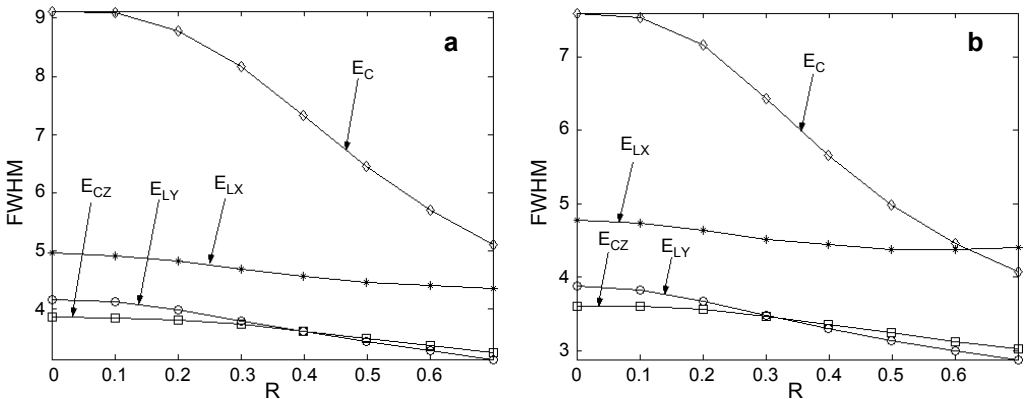

Fig. 1. Transverse FWHM of fields E_{LY}, E_{LX}, E_C, and E_{CZ} under condition of NA = 0.75 (**a**), and NA = 0.80 (**b**).
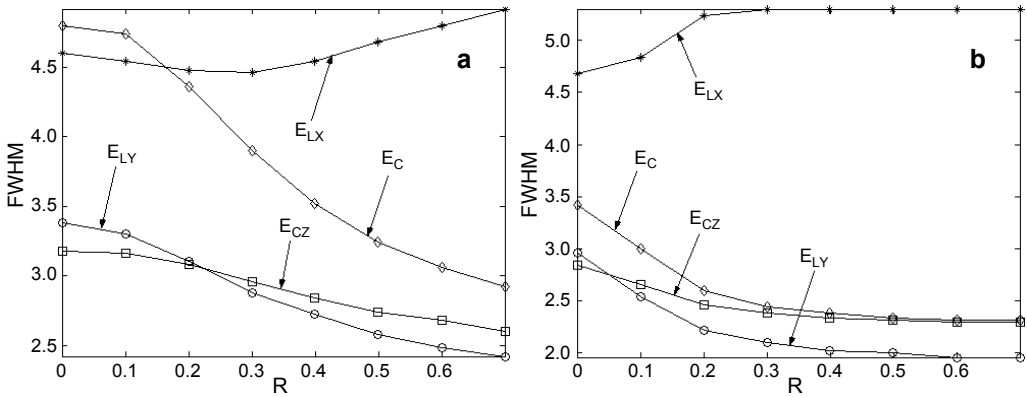
Fig. 2. Transverse FWHM of fields E_{LY}, E_{LX}, E_C, and E_{CZ} under condition of NA = 0.90 (**a**), and NA = 0.99 (**b**).

of E_{LY} and E_{CZ} shifts towards smaller R, comparing Fig. 2**a** and Fig. 1**a**, which means that for larger R, the focal spot of E_{CZ} is actually bigger than that of E_{LY}. Therefore, under condition of higher NA, this critical R value decreases. The range of possibilities of generating smaller focal spot using RPB shrinks if only considering E_{LY} and E_{CZ}. Figure 2**b** shows focusing properties for NA = 0.99. From this figure, we can see that the focal pattern of LPB becomes very asymmetric, and the FWHM difference between E_{LY} and E_{LX} is very significant. The FWHM of E_{LY} is usually smaller than that of E_C and E_{CZ}, and the FWHM difference of E_C and E_{CZ} is not very remarkable.

In order to understand the effect of NA on FWHM, the curves representing the FWHM values upon increasing NA are illustrated in Figs. 3 and 4. We can see from Fig. 3 that the FWHM of E_{LY} is always smaller than that of E_{CZ} under condition of $R = 0$. And for case of $R = 0.1$, two FWHM curves of E_{LY} and E_{CZ} cross each other for certain value of NA, which indicates that the focal size of longitudinal field
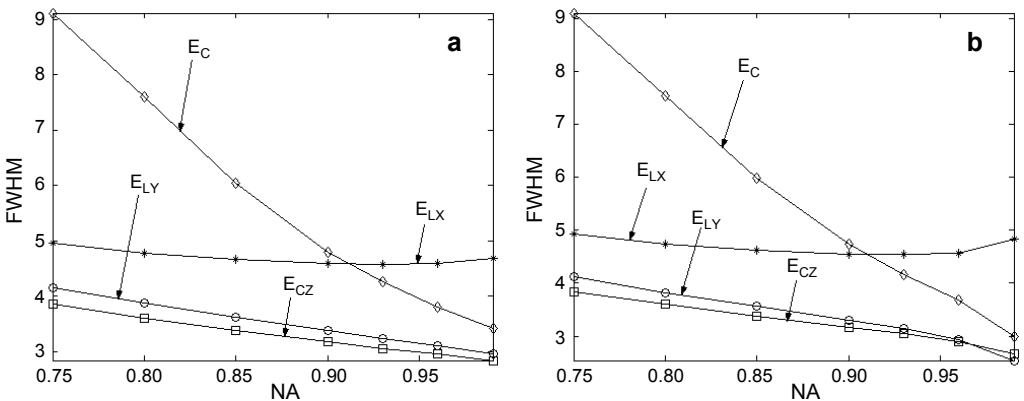

Fig. 3. Transverse FWHM of fields E_{LY}, E_{LX}, E_C, and E_{CZ} under condition of $R = 0.0$ (**a**), and $R = 0.1$ (**b**).

component RPB is not always smaller than that of *y*-axis component of LPB. And for smaller NA, the FWHM of E_C is bigger than that of E_{LX}. However, because the decrease speed of FWHM of E_C is very sharp, the FWHM of E_C becomes smaller than that of E_{LX} for higher NA.

For larger R, the FWHM curves of fields E_{LY}, E_{LX}, E_C, and E_{CZ} on increasing NA are also given in Fig. 4. We can see that the cross point position of FWHM curves of E_{LX} and E_C shifts continuously in decreasing NA direction. And the cross point position of FWHM curves of E_{LX} and E_{CZ} also shifts in decreasing NA direction. When R value ranges from 0.5 to 0.7, the focal spot size of E_{CZ} is actually bigger than that of E_{LY} for the case of changing NA from 0.75 to 0.99, as shown in Figs. 4**b** and 4**c**. Therefore, the effect of NA on the focal size difference between RPB and LPB is very remarkable. The focal spot of RPB is not always smaller than that of LPB. Even if only longitudinal field component is considered, in fact, the condition for tighter focusing of RPB is very complicated.

Some intensity distributions of the polarization components of the focused beams were added. Figure 4 illustrates the intensity distributions of LPB under condition of
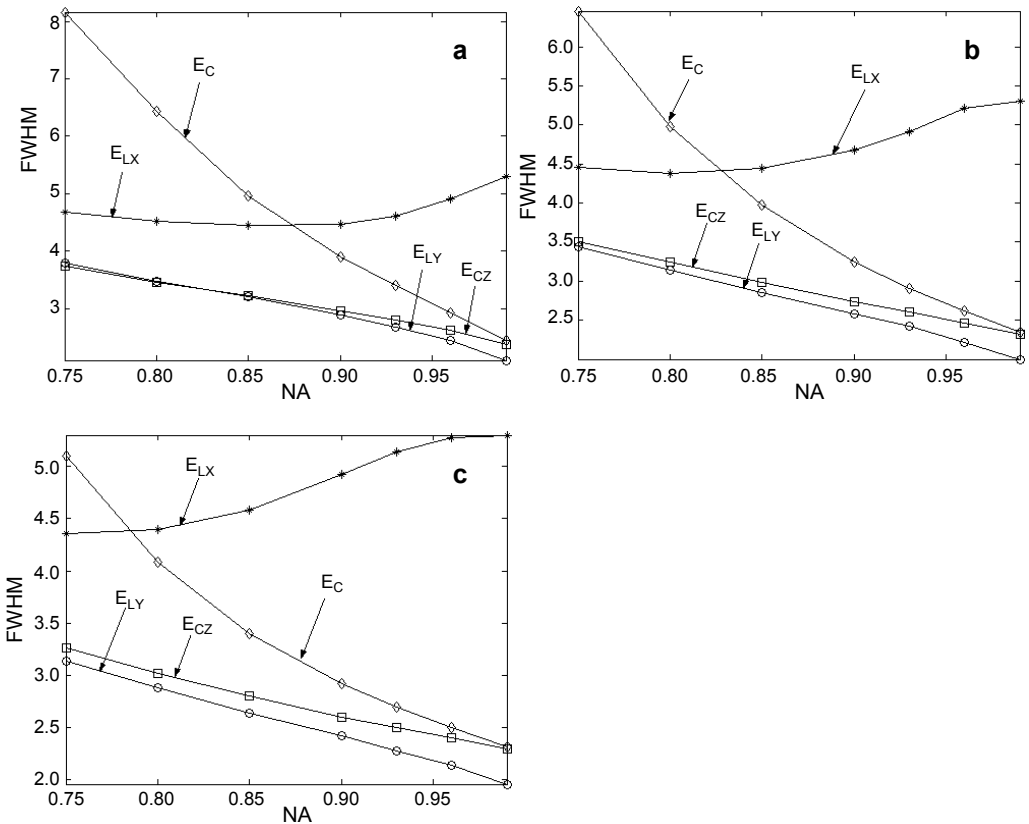

Fig. 4. Transverse FWHM of fields E_{LY}, E_{LX}, E_C, and E_{CZ} under condition of $R = 0.3$ (**a**), $R = 0.5$ (**b**), and $R = 0.7$ (**c**).

$R = 0.2$ and NA = 0.75. And E_x, E_y, and E_z indicate the three polarization components in x, y, z direction, respectively. It can be seen that the total intensity distribution is very similar to that of polarization component of E_x. On increasing NA, the intensity of polarization component of E_z increases considerably, which leads to the extension of the total intensity distribution in x direction, as shown in Fig. 5. Therefore, for certain small R, the circle focal spot extends in x direction for higher NA, which results in the big FWHM of E_{LX}, so the FWHM of E_{LX} decreases, and then increases on increasing NA for small R, and when R becomes big, the FWHM of E_{LX} increases continuously on increasing NA.

Some intensity distributions of the polarization components under condition of larger R are given. It can be seen that the intensity of polarization component of E_z increases considerably on increasing R, comparing Figs. 7 and 8 with Figs. 5 and 6, respectively. And for larger R, the total intensity distribution extends in x direction very remarkably under condition of higher NA, which leads to the focal splits in x direction, as shown in Fig. 8**a**.

All three mutually orthogonal field components occur in the focal region of focusing LPB. Because the intensity distribution shapes the evolution of E_{LX}, on increasing NA, the cross point position of FWHM curves of E_{LX} and E_C shifts continuously in decreasing NA direction. The intensity distribution of the longitudinally polarized component in an axis direction is not rotationally symmetric, which causes the asymmetric deformation of the focal spot. And when annular aperture is
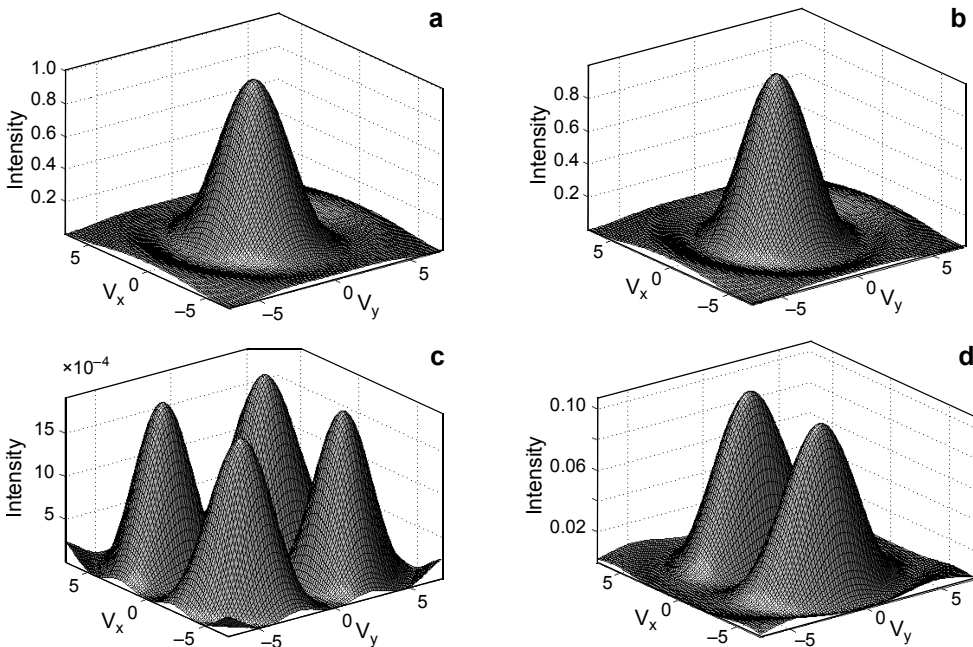

Fig. 5. Intensity distributions of LPB for E (**a**), E_x (**b**), E_y (**c**), and E_z (**d**) under condition of $R = 0.2$ and NA = 0.75.
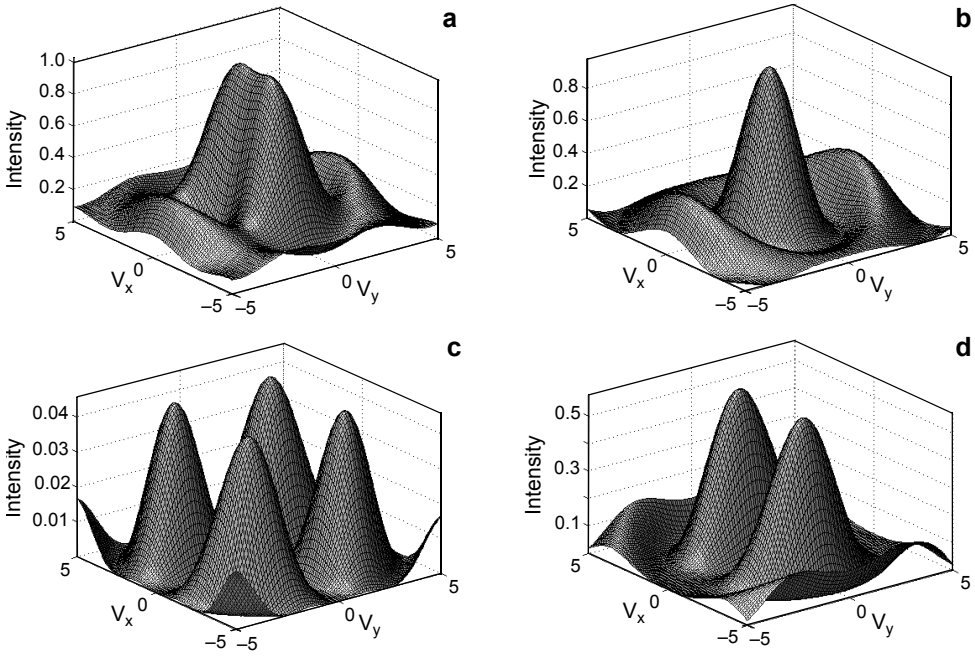
Fig. 6. Intensity distributions of LPB for E (**a**), E_x (**b**), E_y (**c**), and E_z (**d**) under condition of $R = 0.2$ and NA = 0.99.
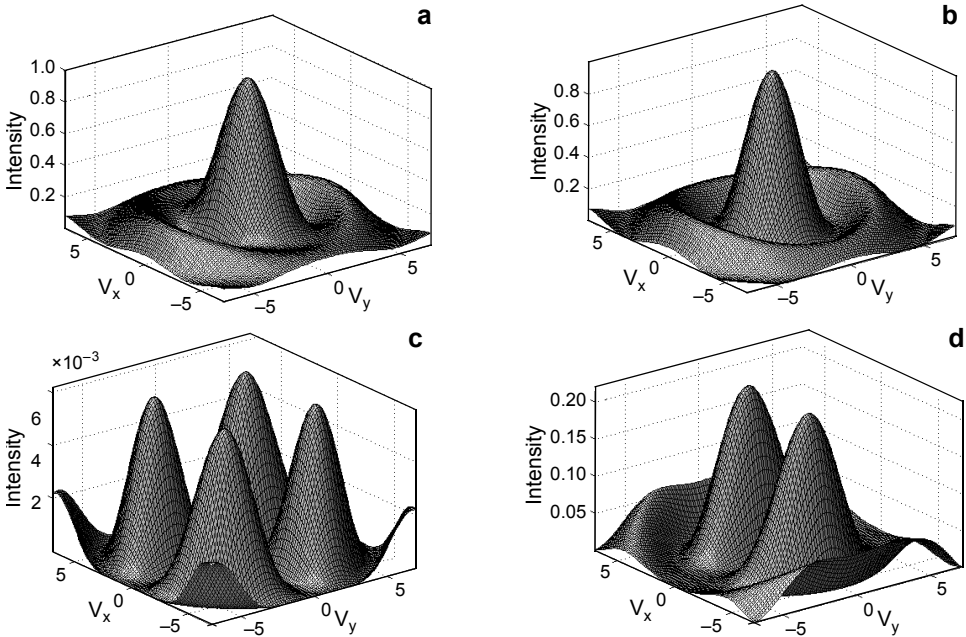
Fig. 7. Intensity distributions of LPB for E (**a**), E_x (**b**), E_y (**c**), and E_z (**d**) under condition of $R = 0.7$ and NA = 0.75.
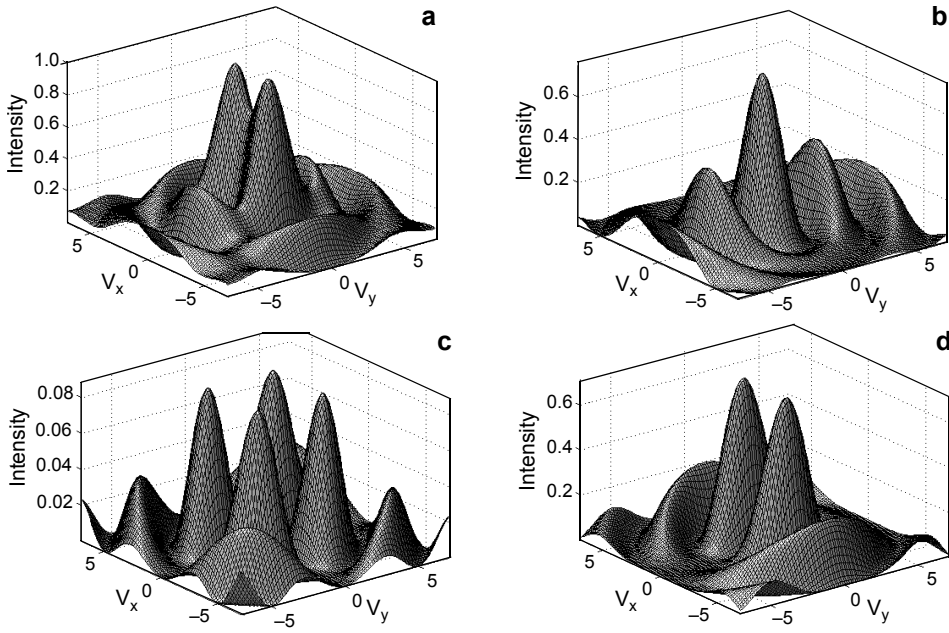
Fig. 8. Intensity distributions of LPB for E (**a**), E_x (**b**), E_y (**c**), and E_z (**d**) under condition of $R = 0.7$ and NA = 0.99.
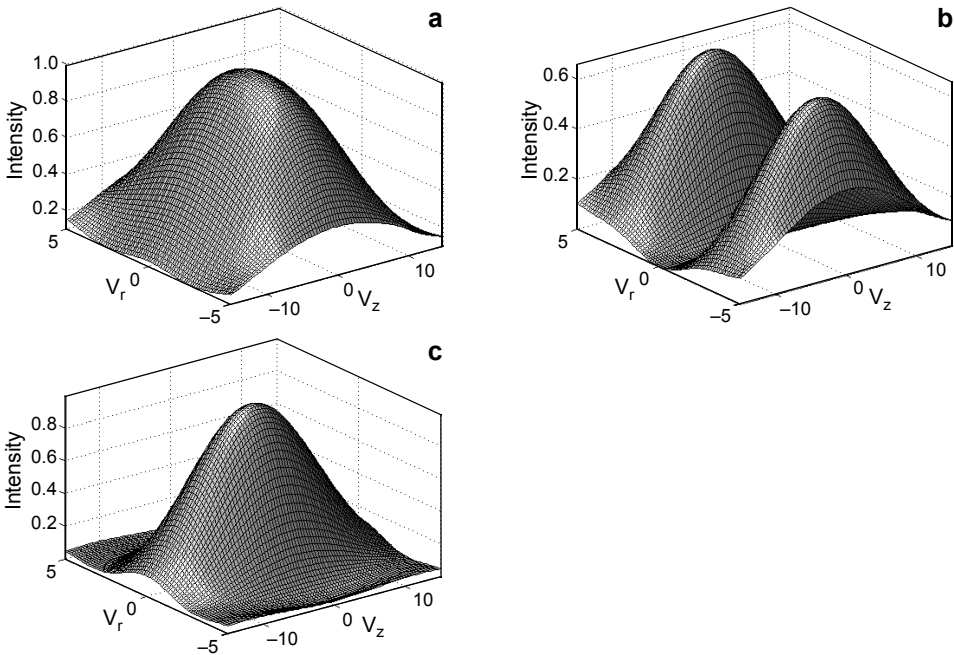

Fig. 9. Intensity distributions of RPB for E (**a**), E_r (**b**), and E_z (**c**) under condition of $R = 0.2$ and NA = 0.75.

used, the relative contribution of the longitudinal component is increased and the asymmetry becomes more considerable. The focal spot splits in transverse direction under condition of larger R. When focal splitting occurs, there are two intensity peaks in focal plane, as shown in Fig. 8. In order to avoid the effect of focal splitting on FWHM of the whole intensity distribution, the maximum value of R is chosen as 0.7.

The intensity distributions of the polarization components of RPB under condition of $R = 0.2$ and NA = 0.75 are also illustrated in Fig. 9. We can see that the transverse size of E_z is smaller than that of the total optical intensity, which leads to the smaller FWHM of field E_{CZ}. And we also know that, in fact, the RPB is often used to obtain smaller focal spot by means of its polarization components in z direction. On increasing NA and R, the polarization component of field E_{CZ} becomes stronger and stronger, which accelerates the focal size decrease of total intensity of RPB.

Therefore, the focal spot evolution of RPB and LPB is different. For the case of focusing of LPB, the focal shape change due to polarization component of E_{LX} is very considerable, even results in focal splitting. While, for the case of focusing of RPB, the field E_{CZ} plays an important role in focusing properties, especially in higher NA and R focusing systems.

3.2. Focal depth comparison between RPB and LPB

Now, we investigate the focal depth of RPB by comparing it with LPB. It should be noted that focal depth is defined as the distance between the two axial points between which the intensity is not smaller than 50% of the intensity peak maximum on optical axis. And by calculating on-axis intensity distributions of RPB and LPB numerically,

T a b l e 2. Focal depth comparison of RPB and LPB under condition of different NA and R.

	NA	0.75	0.80	0.85	0.90	0.93	0.96	0.99
$R = 0$	E_L	16.40	13.94	11.84	10.02	9.02	8.06	7.02
	E_C	17.88	15.12	12.76	10.70	9.54	8.42	7.16
$R = 0.1$	E_L	16.72	14.24	12.16	10.38	9.46	8.66	8.72
	E_C	18.00	15.22	12.88	10.86	9.76	8.76	8.54
$R = 0.2$	E_L	17.68	15.20	13.16	11.52	10.78	10.48	13.14
	E_C	18.58	15.84	13.58	11.72	10.86	10.40	12.90
$R = 0.3$	E_L	19.42	16.90	14.92	13.52	13.10	13.54	19.68
	E_C	20.00	17.10	15.14	13.58	13.08	13.42	19.48
$R = 0.4$	E_L	22.20	19.64	17.74	16.64	16.66	18.12	28.82
	E_C	22.56	19.86	17.82	16.62	16.60	18.00	28.66
$R = 0.5$	E_L	26.52	23.86	20.04	21.38	22.02	24.88	41.86
	E_C	26.74	23.98	20.08	21.34	21.96	24.76	41.74
$R = 0.6$	E_L	33.40	30.56	28.86	28.82	30.36	35.26	61.58
	E_C	33.52	30.64	28.86	28.76	30.30	35.18	61.48
$R = 0.7$	E_L	45.30	40.14	40.58	41.52	44.54	52.84	94.62
	E_C	45.36	40.16	40.58	41.50	44.50	52.78	94.56

the focal depth values under condition of different R and NA are shown in Tab. 2. And E_C and E_L mark RPB and LPB in this table, respectively. The foal depth unit is k^{-1}, where k is the wave number of incident beam.

From this table, it can be seen that the focal depth of RPB also decreases on increasing NA as that of LPB under condition of small R. And focal depth of RPB increases on increasing R, which is also similar to that of LPB. In practice, it is well known that this focal evolution principle is common to LPB, now it is also applicable to focusing RPB. In addition, the focal depth difference between these two kinds of beams also shrinks on increasing NA, and larger R can also result in smaller focal depth difference.

In order to understand the information contained in Tab. 2 more clearly and deeply, the focal depth curves of RPB and LPB on increasing R under condition of different typical NA are illustrated in Fig. 10. We can see from this figure that on increasing R,
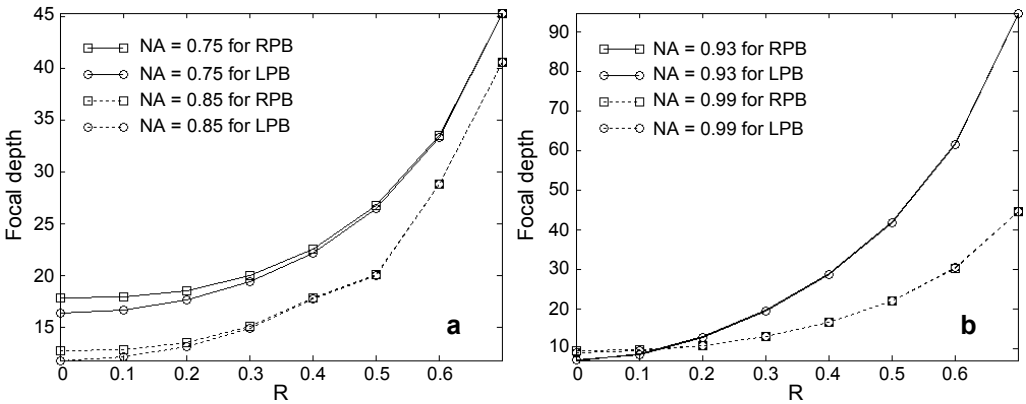

Fig. 10. Focal depth curves of RPB and LPB on increasing R under condition of NA = 0.75, NA = 0.85 (**a**), and NA = 0.93, NA = 0.99 (**b**).
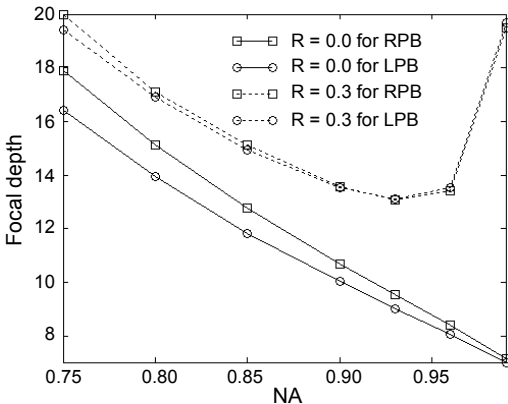

Fig. 11. Focal depth curves of RPB and LPB on increasing NA under condition of different R.

the focal depth increases, while the focal depth difference decreases under condition of NA being the same. And for higher NA, the focal depth difference becomes very slight.

Figure 11 shows focal depth curves of RPB and LPB on increasing NA under condition of two different *R*. The focal depth decreases on increasing NA for smaller *R*. However, when *R* increases, the focal depth decreases firstly for small NA, and then increases sharply when NA is bigger than 0.93. The whole focal evolution process of RPB is similar that of LPB. Here is one sharp increase of focal depth for higher NA and larger *R*.

Figure 12 illustrates the intensity distributions in focal region of the focusing RPB, which shows that the transverse size of longitudinal component is smaller than that of transverse component, while the axial size of longitudinal component is bigger than that of transverse component. Therefore, when the contribution of longitudinal component becomes considerable under condition of larger *R* and higher NA, the focal depth also increases simultaneously.

Extension of the focal depth on increasing *R* may also be explained if the interference of the outermost and innermost rays of the beam axis in the region around the focal point is considered [24]. As KITAMURA and coworkers have shown in reference [24], when the original radially polarized beam is focused, the incident angles
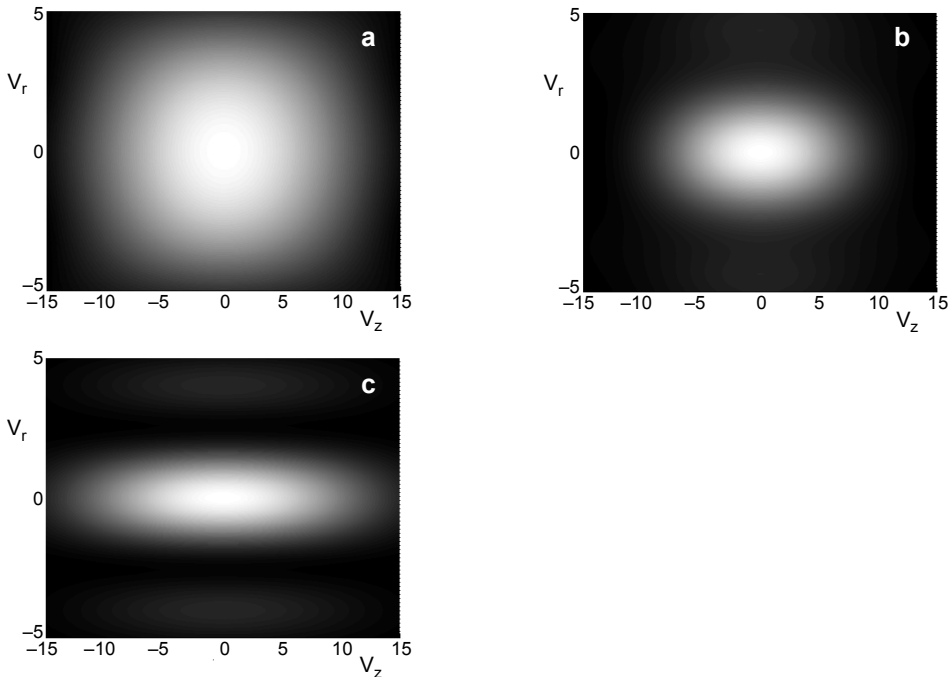

Fig. 12. Intensity distributions of RPB for *R* = 0.3 under condition of NA = 0.75 (**a**), NA = 0.90 (**b**), and NA = 0.99 (**c**).

of the two rays are significantly different. Constructive interference takes place only at the focal plane on the beam axis because the two rays are in phase only at this point. Therefore, strong intensity appears only in close vicinity to the focal plane.

However, the two corresponding rays for the narrow annular incident beam interfere constructively on the beam axis even away from the focal plane, because the phases of the rays match well due to almost identical incident angles. So, the narrower annular incident beam possesses longer focal depth, which is the same cause of focal depth extension for incident LPB and RPB, as shown in Fig. 10. When R is very small or approaches zero, the effect of NA on focal depth is more remarkable than that of annular aperture, so the focal depth decreases on increasing NA, as is well known that the focal depth decreases on increasing NA for clear aperture, for instance, WANG and GAN show that the focal depth is proportional to $1/\text{NA}^2$ [25]. However, when R gets larger, the effect of annular aperture becomes more considerable than that of NA, so the focal depth extends sharply on increasing NA, as shown in Fig. 11.

3.3. Comparison under high-order radial modes

In the case of a single radially polarized doughnut beam, a Bessel–Gaussian beam may be employed, while it was found that the higher-order radially polarized beams are represented by Laguerre–Gaussian distribution [12, 14, 26–28]. In this section, in order to investigate the effect of high-order radial modes on results of Section 3.1, we also choose Laguerre–Gaussian distribution as the amplitude shape of higher-order beams; the distribution can be written as [14, 29],

$$P(r) \; = \; C\exp\!\left(-\frac{r^2}{\omega_0^2}\right)\!\left(2\frac{r^2}{\omega_0^2}\right)^{|l|/2} L_q^l\!\left(\frac{2r^2}{\omega_0^2}\right) \tag{8}$$

where C is constant, r is radial coordinate, and ω_0 is the waist radius. L_q^l represents an associated Laguerre polynomial, and l is the topological charge, q is the radial index. By a similar viable transformation method presented in references [30, 31], the amplitude distribution can be rewritten in the form

$$P(\theta) \; = \; C\exp\!\left(-\frac{\sin^2(\theta)}{w^2\,\text{NA}^2}\right)\!\left(2\,\frac{\sin^2(\theta)}{w^2\,\text{NA}^2}\right)^{|l|/2} L_q^l\!\left(\frac{2\sin^2(\theta)}{w^2\,\text{NA}^2}\right) \tag{9}$$

where w is the radius ratio of waist radius to the radius of optical aperture. NA is the numerical aperture. By substituting Eq. (9) into the Eqs. (2), (3) and Eqs. (5)–(7), the effect of radial variation amplitude on the results presented in Section 3.1 can be investigated numerically.

Figure 13 illustrates the transverse intensity distributions under condition of NA = 0.75, $w = 1$, $l = 1$, and $q = 4$. The horizontal dashed line indicates the half value of the maximum intensity. It can be seen from this figure that the transverse focus size increases on decreasing R. And when the value of R approaches zero, the transverse
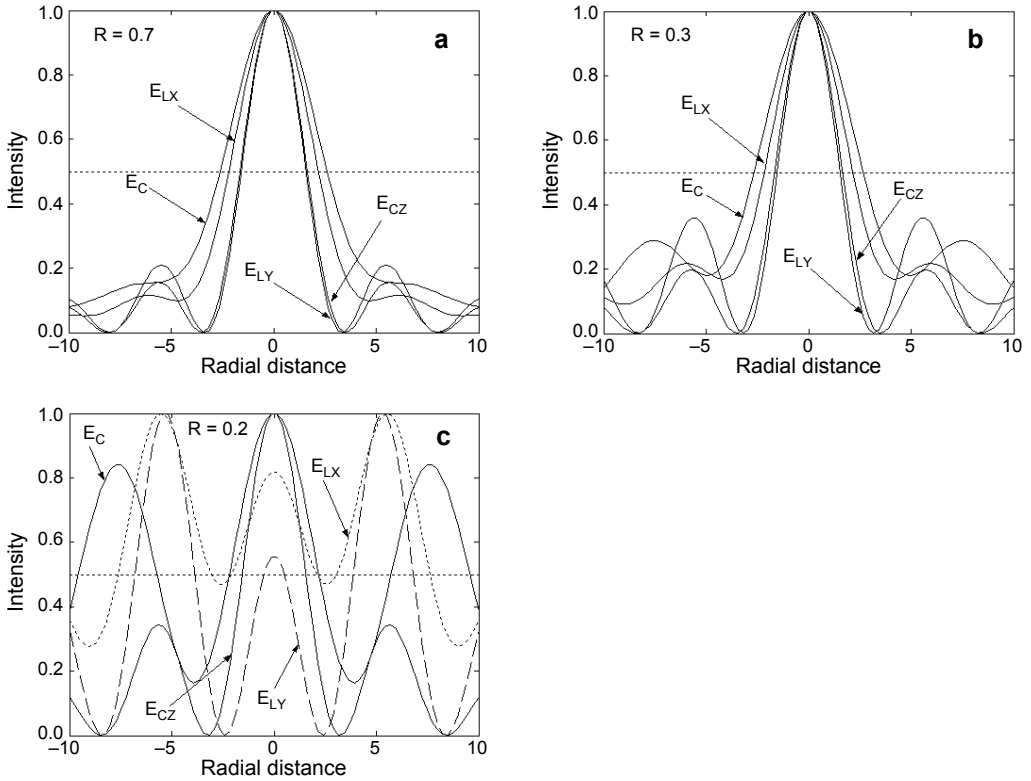
Fig. 13. Transverse intensity distributions under condition of $NA = 0.75$, $w = 1$, $l = 1$, $q = 4$ and $R = 0.7$ (**a**), $R = 0.3$ (**b**), and $R = 0.2$ (**c**).

focal intensity difference becomes very considerable. There is a more pronounced effect of radial variation amplitude for larger apertures (namely, under condition of smaller R). Therefore, we should pay attention to the radial variation amplitude distribution when results in this paper will be used in practical applications.

4. Conclusions

We have investigated tightened focusing of radially polarized beam by comparing it with linearly polarized beam. Numerical results show that the focal spot of radially polarized beam is not always smaller than that of linearly polarized beam. Even it only a longitudinal field component is considered, the condition for tighter focusing of radially polarized vector beam is very complicated. Therefore, more attention should be paid to use of radially polarized beam in practice use for sharper focus according to numerical aperture and the beam shape. The focal depth of focusing annular radially polarized beam is also investigated by comparison with linearly polarized beam. The focal depth of radially polarized beam decreases on increasing numerical aperture like that of linearly polarized beam under condition of small radius ratio, and

increases on increasing radius ratio. Focal depth difference between these two kinds of beams shrinks on increasing numerical aperture. And the larger the radius ratio, the lower the focal depth difference. The above results let us get a deeper insight into the focusing properties of radially polarized beam, and Tabs. 1 and 2 may serve as reference in practice for choosing parameters when radially polarized beam is used in focusing optical systems.

References

[1] Salamin Y.I., *Direct acceleration by two interfering radially polarized laser beams*, Physics Letters A **375**(3), 2011, pp. 795–799.

[2] Youyi Zhuang, Yaoju Zhang, Biaofeng Ding, Taikei Suyama, *Trapping Rayleigh particles using highly focused higher-order radially polarized beams*, Optics Communications **284**(7), 2011, pp. 1734–1739.

[3] Hayazawa N., Saito Y., Kawata S., *Detection and characterization of longitudinal field for tip-enhanced Raman spectroscopy*, Applied Physics Letters **85**(25), 2004, pp. 6239–6241.

[4] Tang W.T., Yew E.Y.S., Sheppard C.J.R., *Polarization conversion in confocal microscopy with radially polarized illumination*, Optics Letters **34**(14), 2009, pp. 2147–2149.

[5] Baohua Jia, Hong Kang, Jiafang Li, Min Gu, *Use of radially polarized beams in three-dimensional photonic crystal fabrication with the two-photon polymerization method*, Optics Letters **34**(13), 2009, pp. 1918–1920.

[6] Kumar A., Gupta M.C., *Laser machining of micro-notches for fatigue life*, Optics and Lasers in Engineering **48**(6), 2010, pp. 690–697.

[7] Xiangping Li, Yaoyu Cao, Min Gu, *Superresolution-focal-volume induced 3.0 Tbytes/disk capacity by focusing a radially polarized beam*, Optics Letters **36**(13), 2011, pp. 2510–2512.

[8] Dorn R., Quabis S., Leuchs G., *Sharper focus for a radially polarized light beam*, Physical Review Letters **91**(23), 2003, article 233901.

[9] Baohua Jia, Xiaosong Gan, Min Gu, *Direct measurement of a radially polarized focused evanescent field facilitated by a single LCD*, Optics Express **13**(18), 2005, pp. 6821–6827.

[10] Xiumin Gao, Mingyu Gao, Song Hu, Hanming Guo, Jian Wang, Songlin Zhuang, *Highly focusing of radially polarized Bessel-modulated Gaussian beam*, Optica Applicata **40**(4), 2010, pp. 965–974.

[11] Xiumin Gao, Mingyu Gao, Qiufang Zhan, Jinsong Li, Hanming Guo, Jian Wang, Songlin Zhuang, *Focal shift in radially polarized hollow Gaussian beam*, Optik – International Journal for Light and Electron Optics **122**(8), 2011, pp. 671–676.

[12] Youngworth K., Brown T., *Focusing of high numerical aperture cylindrical-vector beams*, Optics Express **7**(2), 2000, pp. 77–87.

[13] Kozawa Y., Sato S., *Sharper focal spot formed by higher-order radially polarized laser beams*, Journal of the Optical Society of America A **24**(6), 2007, pp. 1793–1798.

[14] Rashid M., Marago O.M., Jones P.H., *Focusing of high-order cylindrical vector beams*, Journal of Optics A: Pure and Applied Optics **11**(6), 2009, article 065204.

[15] Lerman G.M., Levy U., *Effect on radial polarization and apodization on spot size under tight focusing conditions*, Optics Express **16**(7), 2008, pp. 4567–4581.

[16] Indebetouw G., Bai H., *Imaging with Fresnel zone pupil masks: extended depth of field*, Applied Optics **23**(23), 1984, pp. 4299–4302.

[17] Ojeda-Castaneda J., Landgrave J.E.A., Escamilla H.M., *Annular phase-only mask for high focal depth*, Optics Letters **30**(13), 2005, pp. 1647–1649.

[18] MIKUŁA G., JAROSZEWICZ Z., KOLODZIEJCZYK A., PETELCZYC K., SYPEK M., *Imaging with extended focal depth by means of lenses with radial and angular modulation*, Optics Express **15**(15), 2007, pp. 9184–9193.

[19] SAUCEDA A., OJEDA-CASTAÑEDA J., *High focal depth with fractional-power wave fronts*, Optics Letters **29**(6), 2004, pp. 560–562.

[20] JIE LIN, KE YIN, YUDA LI, JIUBIN TAN, *Achievement of longitudinally polarized focusing with long focal depth by amplitude modulation*, Optics Letters **36**(7), 2011, pp. 1185–1187.

[21] QIWEN ZHAN, LEGER J., *Focus shaping using cylindrical vector beams*, Optics Express **10**(7), 2002, pp. 324–331.

[22] GU M., *Advanced Optical Imaging Theory*, Springer, Heidelberg, 2000.

[23] RICHARDS B., WOLF E., *Electromagnetic Diffraction in optical systems. II. Structure of the image field, aplanatic system*, Proceedings of the Royal Society A **253**(1274), 1959, pp. 358–379.

[24] KITAMURA K., SAKAI K., NODA S., *Sub-wavelength focal spot with long depth of focus generated by radially polarized, narrow-width annular beam*, Optics Express **18**(5), 2010, pp. 4518–4525.

[25] HAIFENG WANG, FUXI GAN, *High focal depth with a pure-phase apodizer*, Applied Optics **40**(31), 2001, pp. 5658–5662.

[26] KOZAWA Y., SATO S., *Focusing property of a double-ring-shaped radially polarized beam*, Optics Letters **31**(6), 2006, pp. 820–822.

[27] TOVAR A.A., *Production and propagation of cylindrically polarized Laguerre–Gaussian laser beams*, Journal of the Optical Society of America A **15**(10), 1998, pp. 2705–2711.

[28] TOVAR A.A., CLARK G.H., *Concentric-circle-grating, surface-emitting laser beam propagation in complex optical systems*, Journal of the Optical Society of America A **14**(12), 1997, pp. 3333–3340.

[29] ARTL J., DHOLAKIA K., ALLEN L., PADGETT M.J., *The production of multiringed Laguerre–Gaussian modes by computer-generated holograms*, Journal of Modern Optics **45**(6), 1998, pp. 1231–1237.

[30] XIUMIN GAO, *Focusing properties of the hyperbolic-cosine-Gaussian beam induced by phase plate*, Physics Letters A **360**(2), 2006, pp. 330–335.

[31] XIUMIN GAO, JINSONG LI, *Focal shift of apodized truncated hyperbolic-cosine-Gaussian beam*, Optics Communications **273**(1), 2007, pp. 21–27.